Reaction Behavior of Stratified SiO_2 Granules during Electrochemical Reduction in Molten $CaCl_2$

Xiao Yang[a], Kouji Yasuda[a,b], Toshiyuki Nohira[a], Rika Hagiwara[a], and Takayuki Homma[c]

[a] Graduate School of Energy Science, Kyoto University, Yoshida-honmachi, Sakyo-ku, Kyoto 606-8501, Japan

[b] Environment, Safety and Health Organization, Kyoto University, Yoshida-honmachi, Sakyo-ku, Kyoto 606-8501, Japan

[c] Faculty of Science and Engineering, Waseda University, 3-4-1 Okubo, Shinjuku-ku, Tokyo 169-8555, Japan

Corresponding author: T. Nohira, nohira@energy.kyoto-u.ac.jp

ABSTRACT

The electrochemical reduction behavior of stratified SiO_2 granules in molten $CaCl_2$ at 1123 K (850℃) was investigated to develop a new process for producing solar-grade silicon. The cross sections of the electrolyzed electrode prepared from a graphite crucible filled with SiO_2 granules were observed and analyzed. The visual and SEM observations indicate that the overall reduction proceeds via two different routes. In one route, the reduction proceeds along the granule surfaces from the SiO_2 near the conductor to the distant SiO_2. In the other route, the reduction proceeds from the granule surface to the core of each granule. The reduction along the granule surfaces is faster than that from the surface to the core. Fine SiO_2 granules are expected to be favorable for a high reduction rate.

Key Words: Solar-grade Silicon, Silica, Electrolysis, Molten Salt

I. INTRODUCTION

The established energy economy, fueled by oil, coal, and natural gas, is being replaced by an economy powered by renewable energies such as solar, wind, and geothermal energy. Of the renewable energy sources, the growth of the solar power industry in the past decade can be described as explosive. According to the latest data released by the European Photovoltaic Industry Association (EPIA), the global cumulative installed solar cell capacity has increased from 2.2 GW in 2002 to 102 GW in 2012.[1] The annual installation of solar cells in the world has reached 28.6 GW in 2012.[2]

Currently, crystalline silicon is the most prevalent raw material for solar cells on the market. Solar cells manufactured with silicon accounted for 88% of the global solar cell production in 2012.[2] It will take several decades before technologies based on other materials will become competitive from a business aspect. With the rapid growth of the solar power industry, the consumption of solar-grade silicon (SOG-Si; 6N purity) has grown dramatically and an average growth of 10–20% per year is estimated for the next decade.

The modified Siemens process, based on the hydrogen reduction and thermal decomposition of trichlorosilane ($SiHCl_3$), is currently the dominating process for SOG-Si production.[4] The productivity of this process is reinforced by the smaller number of distillations of $SiHCl_3$ and higher temperature of the reduction step compared to the conventional Siemens process. Even though the supply currently satisfies the market demand, the productivity limitation of this process will likely

causes a shortage of the SOG-Si supply after production of solar cells exceeds 50–60 GW per year.[4] Moreover, the modified Siemens process has other disadvantages such as low reaction efficiency and high energy consumption. Therefore, development of an eco-friendly production process for SOG-Si with high yield and low cost is required.

Various processes have been developed with the aim of displacing the current SOG-Si production process.[3, 5-9] Electrochemical methods have been investigated as an alternative process for SOG-Si production.[10-13] Typically, silicon is electrodeposited on a cathode in molten salts, and a silicon compound is supplied as the raw material. In another method, silicon is produced on the cathode via electrorefining using a low-purity Si anode as the raw material.

The authors have reported that solid silica (SiO_2) can be electrochemically reduced to Si in $CaCl_2$-based molten salts using the contacting electrode method.[14-21] In this method, SiO_2 is reduced to Si by electrolysis at the three-phase zone of SiO_2/$CaCl_2$/electrode.[14, 15]

$$SiO_2\ (s) + 4e^- \rightarrow Si\ (s) + 2O^{2-} \qquad (1)$$

The byproducts of the O^{2-} ions are removed from the molten salt at the anode, where the CO_x gas evolution occurs when a carbon anode is employed. The electrochemical reaction proceeds mainly as a solid to solid reaction and only partly as a liquid to solid reaction in which Si is electrodeposited from silicate ions formed by dissolution of SiO_2 in the molten salt.[19, 22] This type of method has also been reported by other groups.[23-29] The novelty and simplicity of this method may lead to a

new process for SOG-Si production by combining it with the use of high-purity silica and directional solidification refinement.[20] The present authors have already proved that the impurities in the produced Si can be controlled at a low level when high-purity SiO_2 is used as the raw material.[30]

Recently, the authors also proposed a semi-continuous electrochemical process of reducing powdery or granular SiO_2 to Si in molten $CaCl_2$.[31] In this process, SiO_2 powder or granules are supplied from the top of the electrolysis cell, stratified on the cathode placed at the bottom of the cell, and electrochemically reduced to Si. The produced Si granules are tapped out from the bottom of the cell as a slurry containing molten $CaCl_2$. In a previous study, the reduction behavior of SiO_2 granules was estimated based on the current transient curve during electrolysis. The reduction front would spread much faster on the granule surface than in the inside of each granule. Therefore, the reduced SiO_2 granules, halfway through the electrolysis, should have a core(SiO_2)-shell(Si) structure. However, this reaction model needs to be confirmed by direct observation of the SiO_2 granules after electrolysis at different reduction stages. Moreover, such direct observation would allow for an integrated understanding of the reduction process, including the mechanism and kinetics, which is crucial to scale up the laboratory experiment for industrial production.

In the present study, the electrochemical reduction of SiO_2 granules in molten $CaCl_2$ at 1123 K (850℃) was investigated using a different approach from the previous studies. The cross sections of the electrolyzed electrodes prepared from a graphite crucible filled with SiO_2 granules were

observed and analyzed. An integrated explanation of the reduction behavior of SiO_2 granules in molten $CaCl_2$ was proposed by combining the present results with the previously proposed mechanism for the reduction of an SiO_2 plate[15] and SiO_2 granules.[30]

II. EXPERIMENTAL

An Al_2O_3 crucible (Nikkato Corp., o.d. 90 × i.d. 80 × height 100 mm) charged with 300 g of $CaCl_2$ (Kojundo Chemical Lab. Co., Ltd., 99%) was set inside an SiO_2 vessel and heated to 1123 K (850℃) in a dry Ar atmosphere. The $CaCl_2$ salt was pre-dried under vacuum at 453 K (180℃) for several days and 773 K for one day. A small graphite crucible (Toyo Tanso Co., Ltd., o.d. 13 × i.d. 8 × height 8 mm) was used as the working electrode. As shown in Figure 1, an Al_2O_3 tube (Nikkato Corp., o.d. 8 × i.d. 5 × height 9 mm) was inserted into the graphite crucible to avoid electrical contact between the wall of the crucible and the sample. The crucible and tube were fixed with a nickel wire (Nilaco Corp., dia.1.0 mm, 99%) by threading it into a drilled hole with 1.2 mm in diameter. The nickel wire acts as a current lead as well. Approximately 0.07 g of high purity SiO_2 granules (Taiheiyo Cement Corp.) with two kinds of granule sizes; 0.10–0.25 mm and 1.0–2.0 mm, were charged in the crucible. Electrical contact to SiO_2 was only available through the bottom of the graphite crucible. A glassy carbon rod (Tokai Carbon Co., Ltd., dia. 5.2 mm) was used as the counter electrode.

Fig. 1

The reference electrode was an Ag^+/Ag electrode in which a silver wire (Nilaco Corp., dia.1.0 mm, 99%) was immersed in a $CaCl_2$ melt containing 0.5%AgCl (Wako Pure Chemical Co., Ltd., 99.5%) in a mullite tube (Nikkato Corp., o.d. 6 × i.d. 4 × height 450 mm). The potential of this reference electrode was occasionally checked against a Ca^{2+}/Ca dynamic reference electrode

galvanostatically prepared on a Mo wire (Nilaco Corp., dia.1.0 mm, 99.95%).[21] All the potentials are given with reference to the Ca^{2+}/Ca potential.

After immersing the working electrode in the $CaCl_2$ melt, the potential of the working electrode was set at 0.5 V vs. Ca^{2+}/Ca. After electrolysis for 2 min to 150 min under a dry Ar atmosphere, the working electrode was taken out from the melt and vertically cut into two exact halves with a diamond wheel saw (SBT 650, Meiwafosis Co., Ltd.). The cross sections were photographed by a digital camera (Pentax Ricoh Imaging Co. Ltd., K100D). After washing the cut samples in 1M hydrochloric acid for 8 h to remove the remaining $CaCl_2$, the cross sections were analyzed by SEM (Keyence Corp., VE-8800) and EDX (AMETEK Co., Ltd., EDAX Genesis APEX2). In some cases, the samples were recovered from the crucible after electrolysis, washed in 1M hydrochloric acid for one day, and then successively washed in distilled water for one day. The obtained powdery samples were characterized by XRD (Rigaku Corp., Ultima IV, Cu-$K\alpha$ line).

III. RESULTS AND DISCUSSION

A. Reduction from the Bottom of the Crucible to the Top of the SiO_2 Layer

During the potentiostatic electrolysis, the recorded current stayed around -0.2 A in all cases, which was similar to the blank electrolysis test without SiO_2 granules. Since the total surface area of the graphite crucible (*ca.* 51.2 cm^2) was much larger compared with the valid surface area (*ca.* 0.2 cm^2) for SiO_2 reduction, the current corresponding to the SiO_2 reduction was difficult to be distinguished from the background current. The large background current is mainly contributed by the electrochemical reaction relevant to the residual moisture in the melt. The cross sections of the working electrodes after electrolysis for (a) 2 min, (b) 10 min, (c) 60 min, and (d) 150 min using SiO_2 granules 0.10–0.25 mm in size are shown in Figure 2. A dark layer is observed at the bottom of the crucible for each sample. It grows up from the bottom as the electrolysis time increased. The XRD patterns of the samples, before and after electrolysis for 150 min, shown in Figure 3, confirm that crystalline Si is formed by electrolysis. Thus, the dark layer consists of Si converted from colorless SiO_2. The thickness of the original SiO_2 layer (δ_O) is *ca.* 4.5 mm, as indicted in Figure 2 (a). The thickness of the reduced dark layer (δ_R) for each electrolysis time is also given in the figure. Only a very thin dark layer is noticed after 2 min of electrolysis, while the layer extends to the top of the original SiO_2 layer after 150 min of electrolysis. The growth of the dark layer from the bottom to the top indicates that SiO_2 granules in contact with the bottom are reduced to Si at the beginning of

Fig. 2

Fig. 3

electrolysis. As the new electron pathways of the reduced Si are extended,[15] the reduction proceeds from the bottom of the crucible to the top of the SiO_2 layer.

Figure 4 shows an SEM image of the cross section of the working electrode that appeared in Figure 2(b) after electrolysis for 10 min. The reduced layer (at least the surface of the granule), as indicated in the figure, is easily identified by the morphology of the granules. Three regions, (a) unreduced layer, (b) interlayer between the reduced and unreduced layers, and (c) reduced layer, are magnified in Figure 5. The results of EDX analysis at the positions designated in Figure 5 are listed in Table I. As shown in Figure 5 (a), a granule in the unreduced layer has a dense and rather smooth surface. At the interlayer (Fig. 5 (b)), the morphology is different. The lower part (Pos. 3) of the granule is porous and the upper part is dense. EDX analysis implies that the surface of the lower part has been reduced to Si while the upper part has not. In accordance with the previous studies using SiO_2 plate electrodes,[14, 15] SiO_2 with a dense surface became porous after electrochemical reduction, and a vacant space was formed because of the significant volume decrease from SiO_2 to Si (SiO_2: 27.3 cm^3 mol^{-1} at 1123 K (850℃),[32] Si: 12.1 cm^3 mol^{-1} at 1123 K (850℃)[33]). In the reduced layer (Fig. 5(c)), only porous particles are found, indicating that the granule has been reduced to some extent. The different granule appearances in the three regions suggest propagation of the reduction from the bottom of the crucible directed to the top of the SiO_2 layer. Since both SEM and EDX are surface analysis methods, the reduction degree inside the granules can only be

Fig. 4

Fig.5

analyzed after cutting them.

B. Reduction inside the SiO_2 Granule

In order to investigate the reduction inside the granules, SiO_2 granules with the size of 1.0-2.0 mm were used. Figure 6 shows the cross sections of the working electrodes after electrolysis for (a) 60 min and (b) 150 min. Propagation of the reduction from the bottom of the crucible to the top of the SiO_2 layer is also observed. Figure 7 shows an SEM image of the cross section of the working electrode after electrolysis for 60 min. The cross section was slightly polished before the observation. In Figure 7, several granules are found to have dense cores, and they were proven to be SiO_2 by EDX. Two regions, (a) and (b) in Figure 7, are magnified to observe the reaction interface. The magnified images are shown in Figure 8 and the results of the EDX analysis at the positions designated in Figure 8 are listed in Table II. In both SEM images, a core-shell structure is observed. EDX analysis indicates that the shells are rich in Si (Pos. 2, 3, 4, and 5), and the cores remain SiO_2 (Pos. 1 and 6).

Fig. 6

Fig. 7

Fig. 8

Considering the morphology of the reduced SiO_2 granules in Figure 8, the reduction progress in an SiO_2 granule is schematically illustrated in Figure 9. The reduction first starts at a certain point on the granule surface (Fig. 9(a)), and later proceeds via two routes: along the surface ($R_{surf.}$), or from the surface to the core ($R_{ins.}$) of the granule. The lengths of the solid arrows in Figure 9 represent the reduction rate. The reduction rate is faster along the granule surface than in the core, i.e. the reaction

Fig. 9

front (three-phase zone) spreads faster at the surface compared to the core (Fig. 9(b)). After the entire surface is reduced and the porous Si shell is formed, as shown in Figure 9 (c), the reduction only proceeds inside the granule.

As reported in previous studies using an SiO_2 plate,[15] or pellets,[21] the reduction rate is thought to be closely related to the diffusion of the O^{2-} ions. The observed reduction behavior is explained by the diffusion rate of O^{2-} ions as follows. As shown in Figure 9, O^{2-} ions are formed both at the granule surface ($O^{2-}_{surf.}$) and inside ($O^{2-}_{ins.}$). The widths of the open arrows in Figure 9 represent the diffusion rate of the O^{2-} ions. For the reduction along the granule surface, the formed O^{2-} ions immediately diffuse into the bulk $CaCl_2$. For the reduction inside, the formed O^{2-} ions initially diffuse through the crevice of Si shell where $CaCl_2$ penetrates and successively to the bulk $CaCl_2$. As explained in the previous study,[15] the O^{2-} ions accumulate in the $CaCl_2$ in the crevice, leading to an increase in the viscosity of $CaCl_2$ and the decrease in the diffusion coefficient of the O^{2-} ions. Consequently, the diffusion of O^{2-} ions decelerates inside the granule compared to the granule surface, resulting in a faster reduction along the granule surface than in the core. Accordingly, the reduction rate is expected to be higher for the smaller SiO_2 granules with a larger total surface area and shorter diffusion path. A detailed explanation of the effect of SiO_2 granule size on the reduction rate will be given in another paper.

C. Reduction Mechanism

By combining the present results with the previously reported mechanism for the reduction of an SiO_2 plate[15] and the predicted mechanism for SiO_2 granules,[31] an integrated explanation of the reduction behavior of SiO_2 granules stratified on the conductor in molten $CaCl_2$ was summarized and is shown in Figure 10.

Fig. 10

(a) The granule surfaces in contact with the conductor are reduced to Si. The initial interface becomes porous because of the volume shrinkage from SiO_2 to Si. Molten $CaCl_2$ penetrates into the formed crevices, and the byproduct O^{2-} ions diffuse away towards the anode. The produced Si with a high electric conductivity at 1123 K (850 ℃)[34] forms new three-phase (SiO_2/$CaCl_2$/Si) zones.

(b) With the creation of new three-phase zones, the reduction proceeds both along the SiO_2 granule surface and into the core. The reduction is faster in the surface region compared to the inside region because of the difference in the diffusion rate of the O^{2-} ions.

(c) A porous shell of Si is formed while the core remains unreacted for the SiO_2 granules in contact with the conductor. Since electrons are supplied through the porous Si shell, the reduction also proceeds at the SiO_2 granules second neighbor to the conductor.

(d) The reduction proceeds via two routes: (1) from the SiO_2 granules near the conductor to the top of the SiO_2 layer along the granule surfaces, and (2) from the surface to the core in partially

reduced granules.

IV. CONCLUSIONS

The electrochemical reduction behavior of SiO_2 granules stratified on the current collector graphite in molten $CaCl_2$ at 1123 K (850℃) was investigated. The results show that the overall reduction proceeds via two different routes. One route is from the SiO_2 granules near the conductor to the distant ones along the granule surfaces. The other is from the surface to the core in partially reduced granules. The results also indicate that the reduction is faster via the former route rather than the latter one. The overall reduction rate is expected to improve using fine SiO_2 granules.

ACKNOWLEDGMENTS

This study was partly supported by JST-CREST and Grants-in-Aid for Scientific Research A from the Japan Society for the Promotion of Science (JSPS). We thank Taiheiyo Cement Corporation for providing high purity SiO_2 granules.

REFERENCES

[1] *Global market outlook for photovoltaics 2013-2017*, European Photovoltaic Industry Association, Brussels, May 2013.

[2] *Rare Metal News*, Arumu Publishing Co., Tokyo, June 16, 2013.

[3] H. Oda: *Kogyo Zairyo*, 2007, vol. 55, pp. 30-34.

[4] *Industrial Rare Metal 2012, vol. 128*, Arumu Publishing Co., Tokyo, 2012.

[5] K. Yasuda and T. H. Okabe: *JOM*, 2010, vol. 62, pp. 94-101.

[6] K. Yasuda, K. Saegusa, and T. H. Okabe: *Metall. Mater. Trans. B*, 2011, vol. 42, pp. 37-49.

[7] T. Yoshikawa and K. Morita: *JOM*, 2012, vol. 64, pp. 946-951.

[8] J. Sanchez, J. Barona, E. Conejero, M. Canle, X. Rel, P. Garcia, and M. Martinez: U.S. Patent, US008168123B2, 2012.

[9] B. G. Gribov and K. V. Zinov'ev: *Inorg. Mater.* 2003, vol. 39, pp. 653-662.

[10] D. Elwell and R. S. Feigelson: *Sol. Energy Mater.*, 1982, vol. 6, pp. 123-145.

[11] D. Elwell and G. M. Rao: *J. Appl. Electrochem.*, 1988, vol. 18, pp. 15-22.

[12] J. Olson and K. Carleton: *J. Electrochem. Soc.*, 1981, vol. 128, pp. 2698-2699.

[13] J. Cai, X. Luo, G. M. Haarberg, O. E. Kongstein, and S. Wang: *J. Electrochem. Soc.*, 2012, vol. 159, pp. D155-D158.

[14] T. Nohira, K. Yasuda, and Y. Ito: *Nat. Mater.*, 2003, vol. 2, pp.397-401.

[15] K. Yasuda, T. Nohira, K. Amezawa, Y. H. Ogata, and Y. Ito: *J. Electrochem. Soc.*, 2005, vol. 152, pp. D69-D74.

[16] K. Yasuda, T. Nohira, Y. H. Ogata, and Y. Ito: *Electrochim. Acta*, 2005, vol. 51, pp. 561-565.

[17] K. Yasuda, T. Nohira, and Y. Ito: *J. Phys. Chem. Solids*, 2005, vol. 66, pp. 443-447.

[18] K. Yasuda, T. Nohira, Y. H. Ogata, and Y. Ito: *J. Electrochem. Soc.*, 2005, vol. 152, pp. D208-D212.

[19] K. Yasuda, T. Nohira, R. Hagiwara, and Y. H. Ogata: *J. Electrochem. Soc.*, 2007, vol. 154, pp. E95-E101.

[20] K. Yasuda, T. Nohira, R. Hagiwara, and Y. H. Ogata: *Electrochim. Acta*, 2007, vol. 53, pp. 106-110.

[21] K. Yasuda, T. Nohira, K. Takahashi, R. Hagiwara, and Y. H. Ogata: *J. Electrochem. Soc.*, 2005, vol.152, pp. D232-D237.

[22] W. Xiao, X. Wang, H. Yin, H. Zhu, X. Mao, and D. Wang: *RSC Advances*, 2012, vol. 2, pp. 7588-7593.

[23] X. Jin, P. Gao, D. Wang, X. Hu, and G. Z. Chen: *Angewandte Chemie*, 2004, vol. 116, pp. 751-754.

[24] P. C. Pistorius and D. J. Fray: *J. S. Afr. Inst. Min. Metall.*, 2006, vol. 106, pp. 31-41.

[25] W. Xiao, X. Jin, Y. Deng, D. Wang, X. Hu, and G. Z. Chen: *ChemPhysChem.*, 2006, vol. 7, pp.

1750-1758.

[26] W. Xiao, X. Jin, Y. Deng, D. Wang, X. Hu, and G. Z. Chen: *J. Electroanal. Chem.*, 2010, vol. 639, pp. 130-140.

[27] S. K. Cho, F. F. Fan, and A. J. Bard: *Electrochim. Acta*, 2012, vol. 65, pp. 57-63.

[28] Y. Jiang, J. Xu, X. Guan, U.B. Pal, and S.N. Basu: MRS Proceedings, 2012, vol. 1493, pp 231-235.

[29] T. Oishi, M. Watanabe, K. Koyama, M. Tanaka, and K. Saegusa: *J. Electrochem. Soc.*, 2011, vol. 158, pp. E93-E99.

[30] K. Yasuda, T. Nohira, K. Kobayashi, N. Kani, T. Tsuda, and R. Hagiwara: *Energy Technology*, 2013, vol. 1, pp. 245-252.

[31] T. Toba, K. Yasuda, T. Nohira, X. Yang, R. Hagiwara, K. Ichitsubo, K. Masuda, and T. Homma: *Electrochem.*, 2013, vol. 81, pp. 559-565.

[32] T. Kagami and A. Hayashi: *Product and Application of High-purity Silica*, CMC Publ., Tokyo, 1991.

[33] Y. Okada and Y. Tokumaru: *J. Appl. Phys.*,1984, vol. 56, pp. 314-320.

[34] G. L. Pearson and J. Bardeen: *Phy. Rev.*, 1949, vol. 75, pp. 865-883.

Caption List

Table I. Results of the EDX analysis of the positions in Fig. 5.

Table II. Results of the EDX analysis of the positions in Fig. 8.

Figure 1. Schematic illustration of the working electrode structure.

Figure 2. Photographs of the cross sections of the working electrodes after electrolysis at 0.5 V vs. Ca^{2+}/Ca for 2 min to 150 min in molten $CaCl_2$ at 1123 K (850℃). SiO_2 size: 0.10–0.25 mm.(δ_R—thickness of the reduced dark layer; δ_O—thickness of the original SiO_2 layer)

Figure 3. XRD patterns of (a) raw SiO_2 and (b) the sample after electrolysis at 0.5 V vs. Ca^{2+}/Ca for 150 min in molten $CaCl_2$ at 1123 K (850℃).

Figure 4. SEM image of the cross section of the working electrode after electrolysis at 0.5 V vs. Ca^{2+}/Ca for 10 min in molten $CaCl_2$ at 1123 K (850℃). SiO_2 size: 0.10–0.25 mm.

Figure 5. Magnified SEM images of the regions shown in Fig. 4.

Figure 6. Photographs of the cross sections of the working electrodes after electrolysis at 0.5 V vs. Ca^{2+}/Ca for 60 min and 150 min in molten $CaCl_2$ at 1123 K (850℃). SiO_2 size: 1.0–2.0 mm.

Figure 7. SEM image of the cross section of the working electrode after electrolysis at 0.5 V vs.

Ca^{2+}/Ca for 60 min in molten $CaCl_2$ at 1123 K (850℃). SiO_2 size: 1.0–2.0 mm.

Figure 8. Magnified SEM images of the regions shown in Fig. 7.

Figure 9. Schematic illustration of the reduction progress in an SiO_2 granule. ($R_{surf.}$—reduction along the surface, $R_{ins.}$—reduction from the surface to core, $O^{2-}_{surf.}$—O^{2-} ions formed at the granule surface, $O^{2-}_{ins.}$—O^{2-} ions formed inside the granule)

Figure 10. Schematic illustration of the mechanism of electrochemical reduction of SiO_2 granules in molten $CaCl_2$.

Table I. Results of the EDX analysis of the positions in Fig. 5.

Position	Concentration (at%)				
	Si	O	Ca	Cl	C
1	31.2	64.9	0.3	-	3.6
2	29.8	63.3	0.3	0.8	5.8
3	72.7	21.2	1.4	0.7	4.0
4	70.8	29.2	-	-	-
5	76.6	17.6	1.0	0.9	3.9

-: Not detected

Table II. Results of the EDX analysis of the positions in Fig. 8.

Position	Concentration (at%)				
	Si	O	Ca	Cl	C
1	33.6	60.9	0.5	-	5.0
2	66.5	24.6	1.0	1.3	6.6
3	68.6	26.5	0.9	0.6	3.4
4	81.7	15.0	-	-	3.3
5	74.7	19.4	-	0.8	5.1
6	26.2	68.7	0.3	-	4.8

-: Not detected

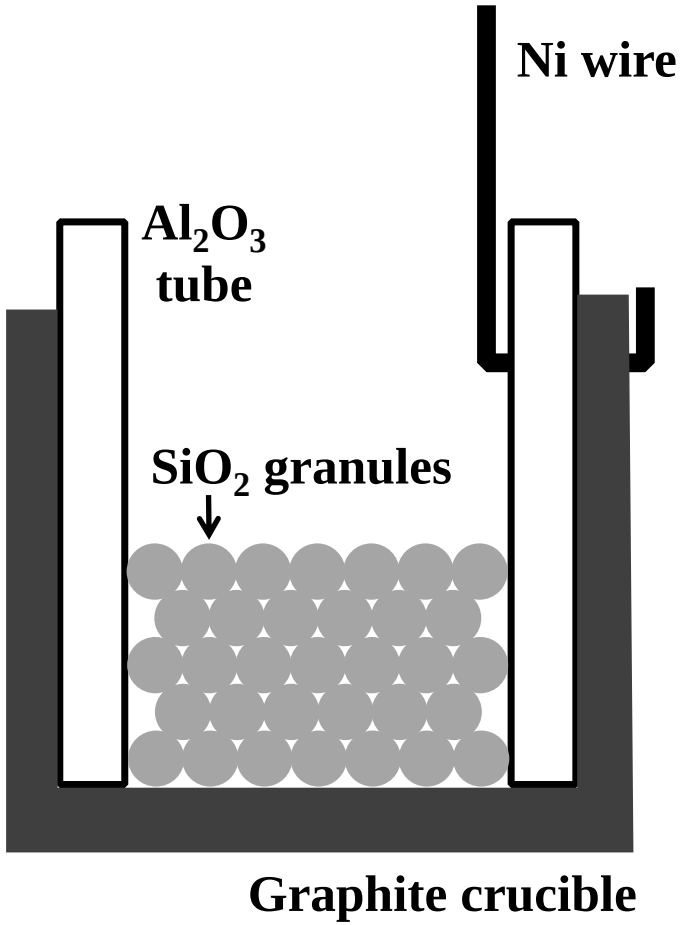

Fig. 1 Schematic illustration of the working electrode structure.

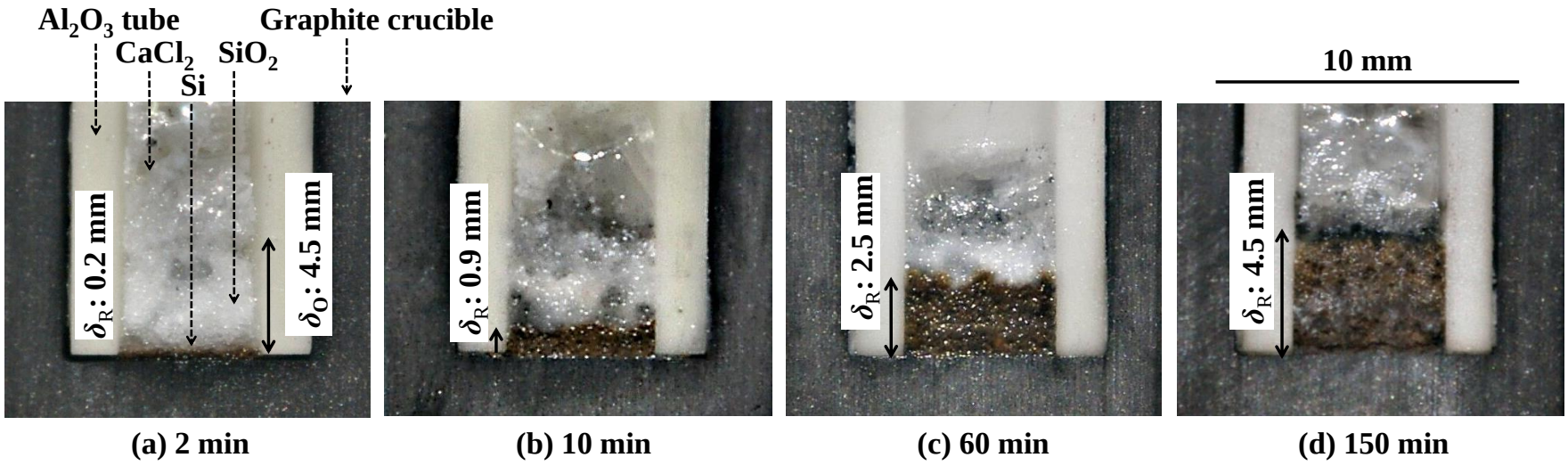

Fig. 2 Photographs of the cross sections of the working electrodes after electrolysis at 0.5 V vs. Ca^{2+}/Ca for 2 min to 150 min in molten $CaCl_2$ at 1123 K. SiO_2 size: 0.10–0.25 mm. (δ_R—thickness of the reduced dark layer; δ_O—thickness of the original SiO_2 layer)

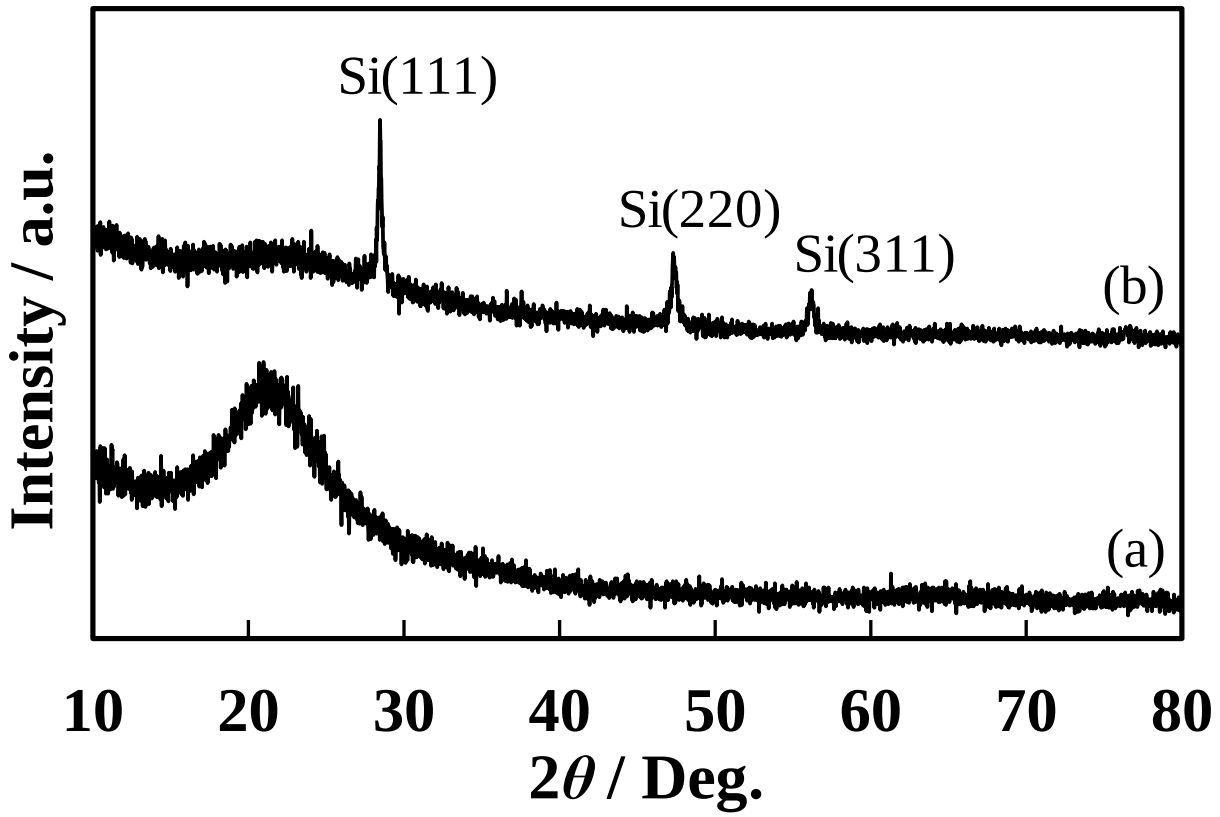

Fig. 3 XRD patterns of (a) raw SiO_2 and (b) the sample after electrolysis at 0.5 V vs. Ca^{2+}/Ca for 150 min in molten $CaCl_2$ at 1123 K.

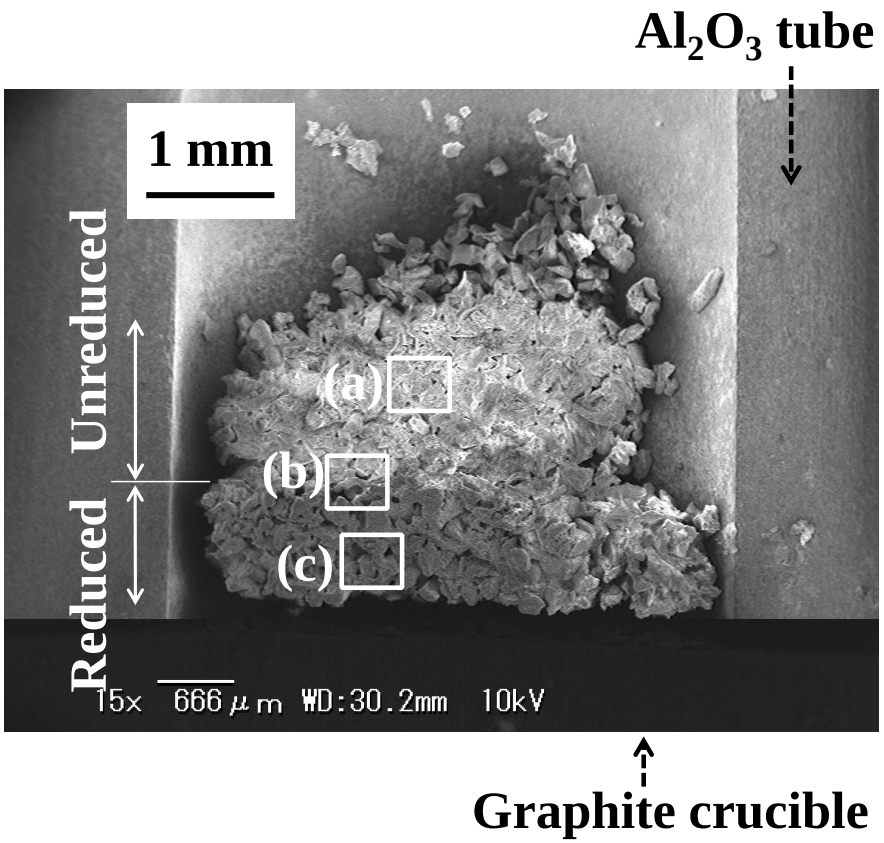

Fig. 4 SEM image of the cross section of the working electrode after electrolysis at 0.5 V vs. Ca^{2+}/Ca for 10 min in molten $CaCl_2$ at 1123 K. SiO_2 size: 0.10–0.25 mm.

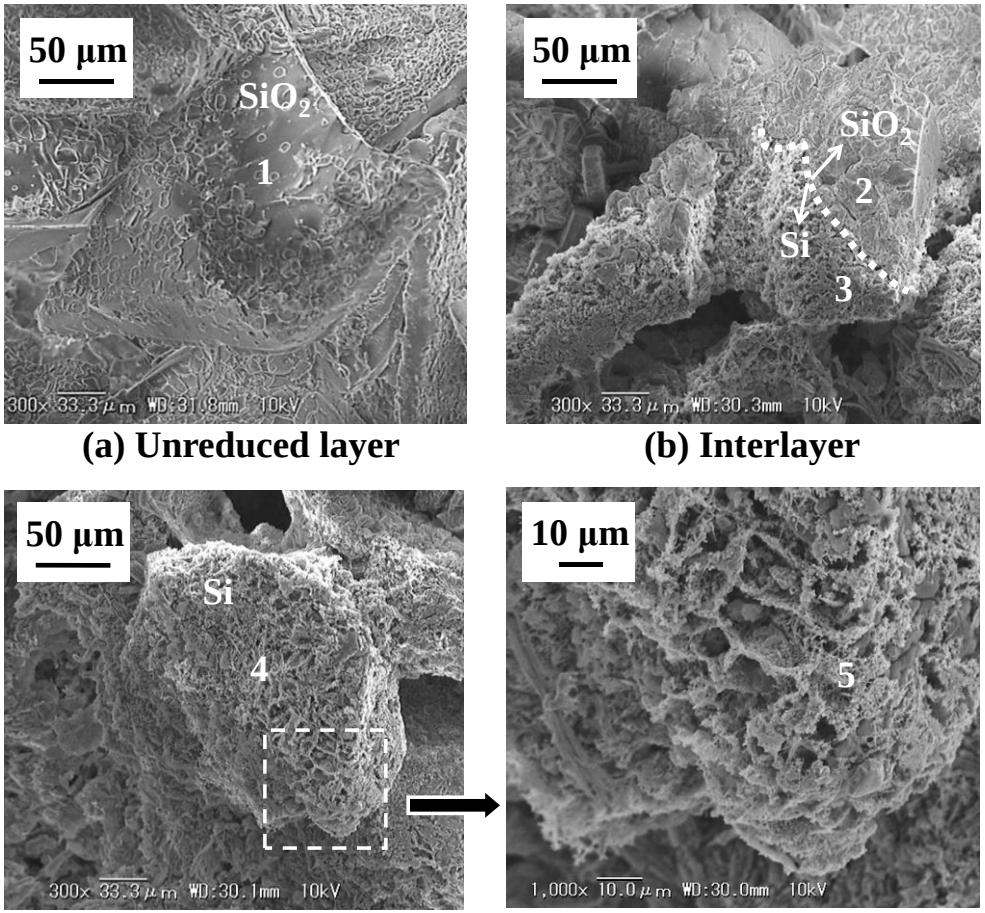

Fig. 5 Magnified SEM images of the regions shown in Fig. 4.

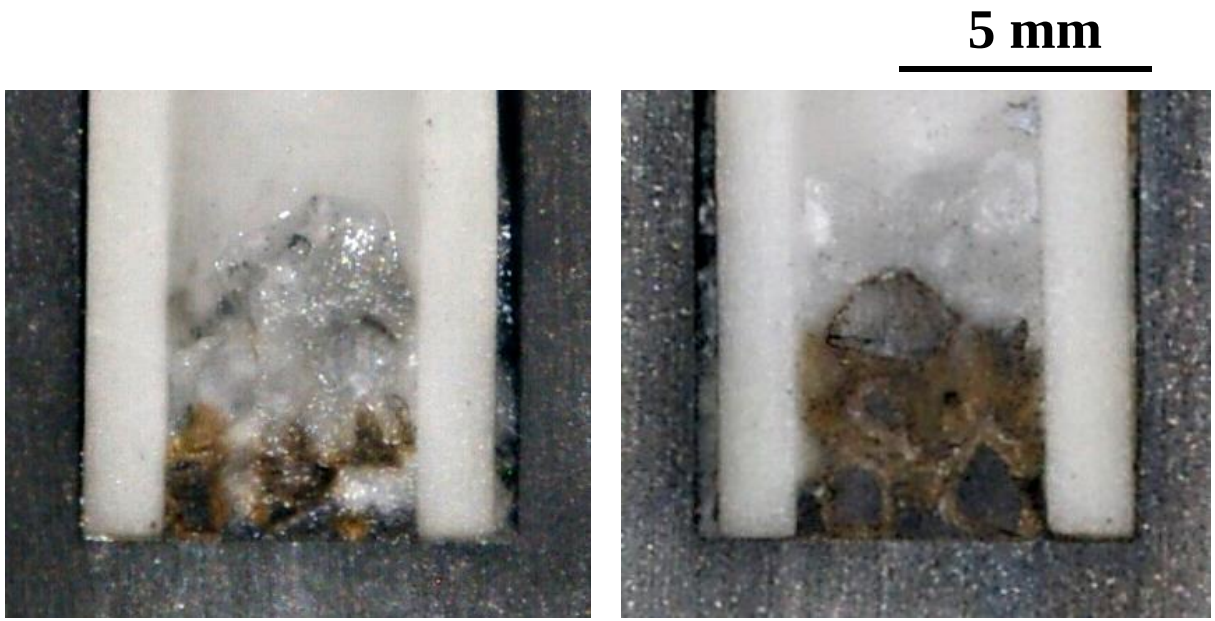

Fig. 6 Photographs of the cross sections of the working electrodes after electrolysis at 0.5 V vs. Ca^{2+}/Ca for 60 min and 150 min in molten $CaCl_2$ at 1123 K. SiO_2 size: 1.0–2.0 mm.

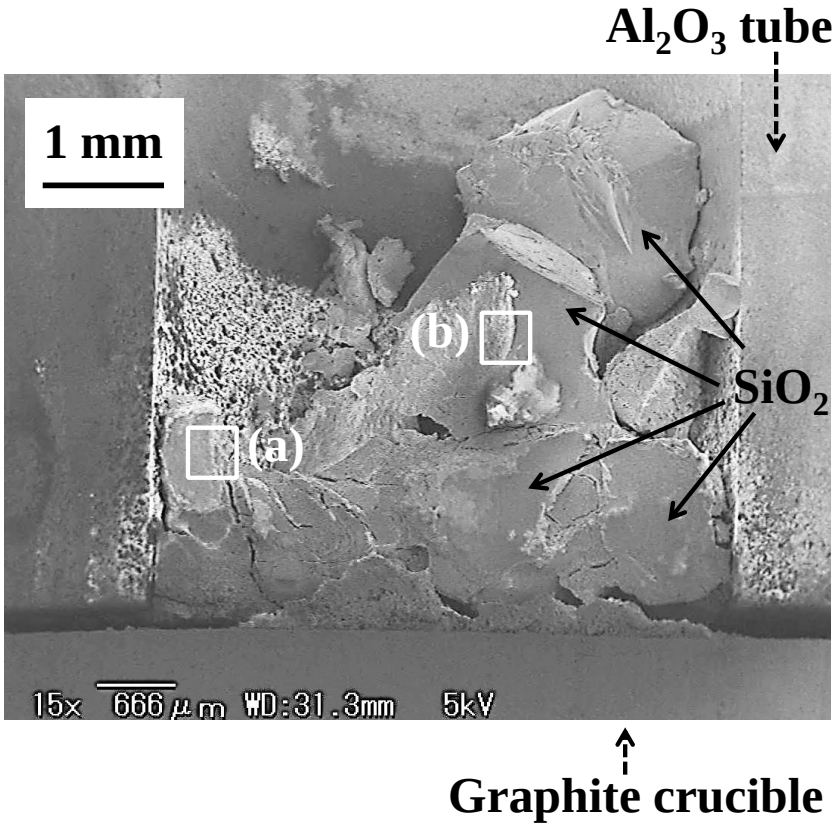

Fig. 7 SEM image of the cross section of the working electrode after electrolysis at 0.5 V vs. Ca^{2+}/Ca for 60 min in molten $CaCl_2$ at 1123 K. SiO_2 size: 1.0–2.0 mm.

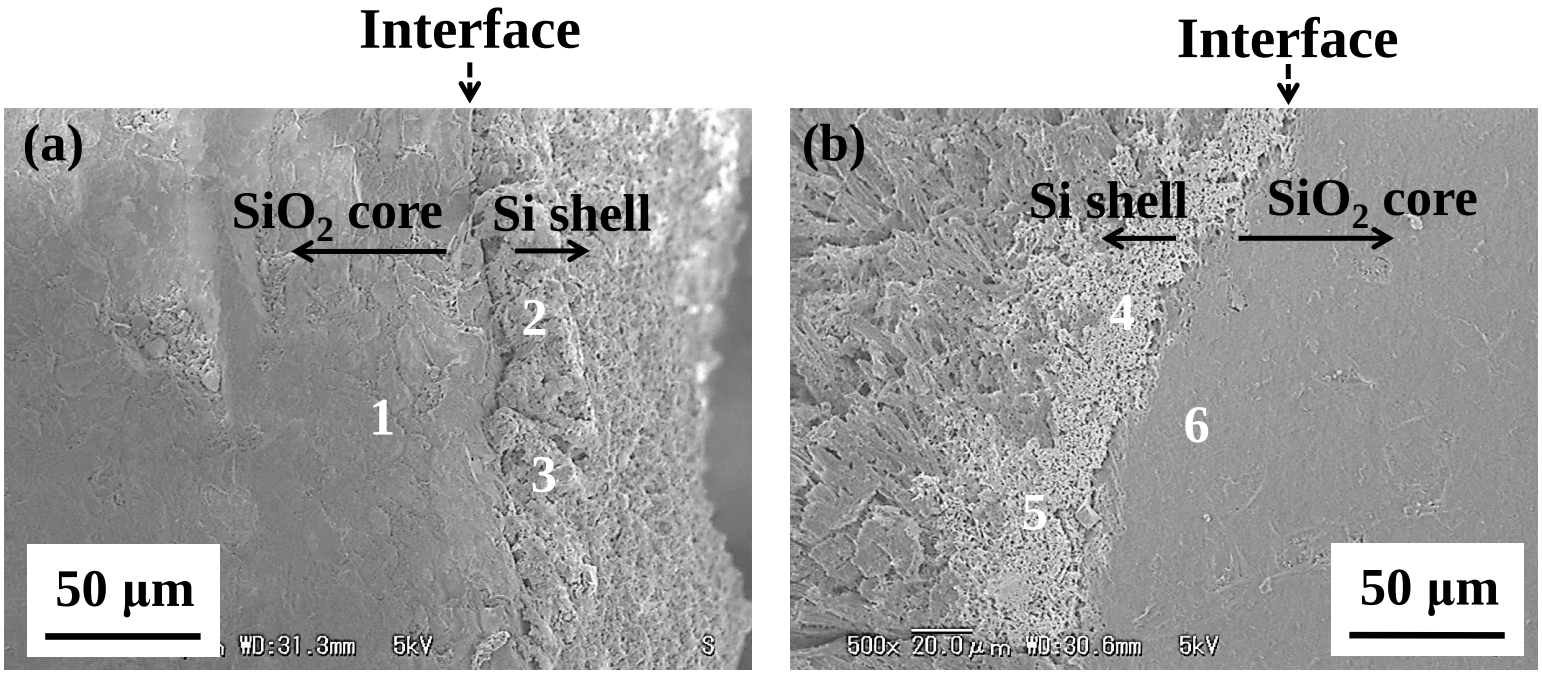

Fig. 8 Magnified SEM images of the regions shown in Fig. 7.

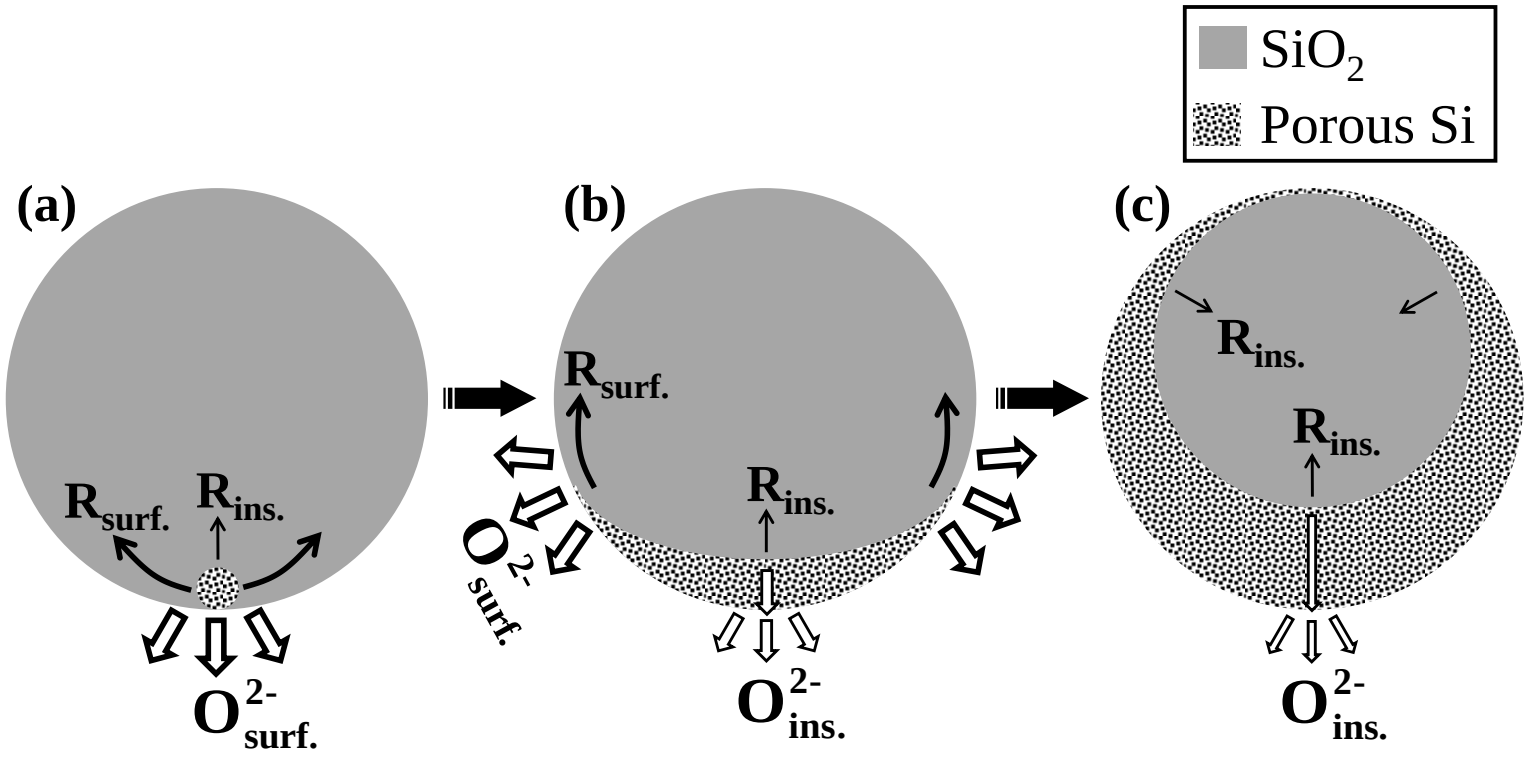

Fig. 9 Schematic illustration of the reduction progress in an SiO_2 granule.

($R_{surf.}$—reduction along the surface, $R_{ins.}$—reduction from the surface to core, $O^{2-}_{surf.}$—O^{2-} ions formed at the granule surface, $O^{2-}_{ins.}$—O^{2-} ions formed inside the granule)

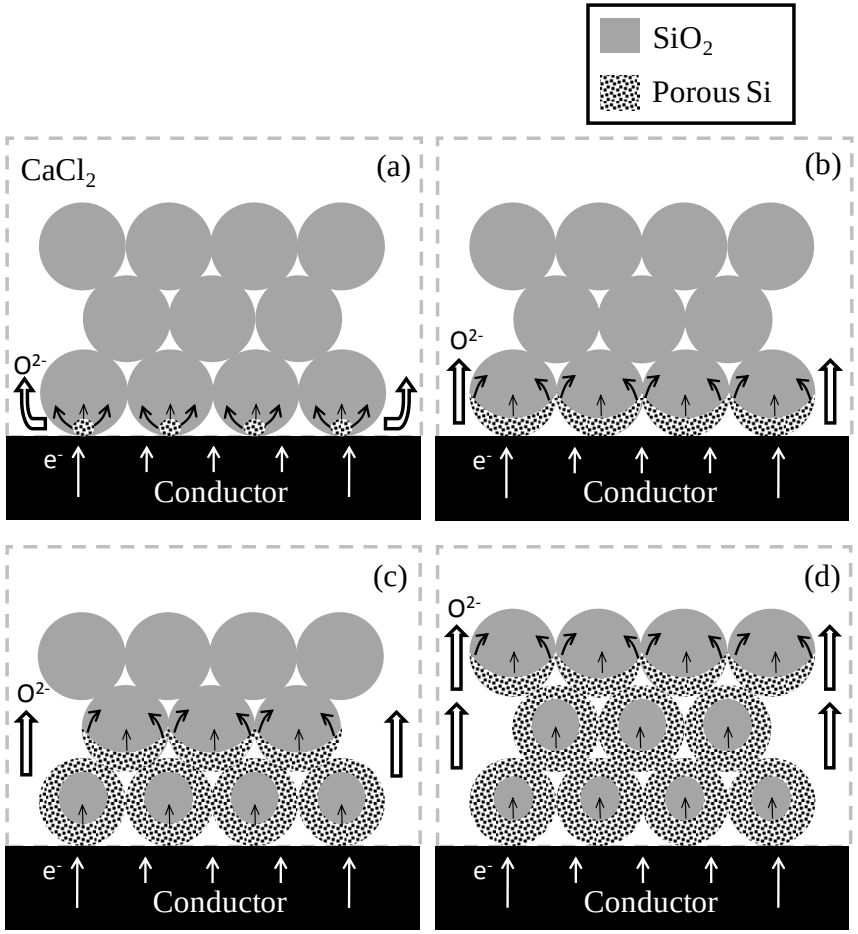

Fig. 10 Schematic illustration of the mechanism of electrochemical reduction of SiO_2 granules in molten $CaCl_2$.